Supplement of Atmos. Chem. Phys., 23, 13235–13253, 2023
https://doi.org/10.5194/acp-23-13235-2023-supplement

Atmospheric Chemistry and Physics
Open Access
EGU

Supplement of

Investigation of the summer 2018 European ozone air pollution episodes using novel satellite data and modelling

Richard J. Pope et al.

Correspondence to: Richard J. Pope (r.j.pope@leeds.ac.uk)

Supplement

Supplementary Material (SM) 1 – Satellite Ozone Averaging Kernels

This work has used satellite sub-column tropospheric ozone (SCO_3, surface – 450 hPa) data produced by RAL from the Global Ozone Monitoring Experiment – 2 (GOME-2) and by their extended Infrared and Microwave Sounding (IMS) scheme applied to IASI, MHS and AMSU on MetOp-A. For each of these products, **Figure S1** shows averaging kernels (AKs) for the 1st June 2017 and 2018 averaged over the European domain. The AK shows the sensitivity of the retrieved profile at different levels to a perturbation in the true profile at different levels (Rodgers, 2000; Eskes and Boersma, 2003). Therefore, it represents the instrument's vertical sensitivity to retrieving ozone. For both GOME-2 and IMS, AK shapes show that retrieval levels at lower altitudes have sensitivity to troposphere ozone. The degree of freedom of signal (DOFS) for SCO_3 for GOME-2 is 0.45 while IMS ranges between 0.62 and 0.65. Therefore, there is good information in these products on SCO_3, which remains similar between the two years, so we are justified in using these SCO_3 products in this study.

Supplementary Material (SM) 2 – Ozone Precursor Gases

The enhancements in tropospheric ozone (O_3) in the summer of 2018 across Europe, as presented in the main manuscript, are likely to be driven by a combination of factors because tropospheric O_3 distributions are influenced by precursor emissions, meteorological conditions, deposition, stratospheric intrusion and atmospheric chemistry. Therefore, we explore how several precursor gases methanol (CH_3OH), nitrogen dioxide (NO_2) and carbon monoxide (CO), which also can be observed by satellite, compare between the summers of 2017 and 2018. **Figure S2** compares total column CH_3OH ($TCCH_3OH$) amounts for May to August in 2017 and 2018 retrieved by RAL's extended IMS scheme applied to MetOp-A data from IASI, MHS and AMSU. In 2017, the peak column values occur in July (10.0-15.0×10^{15} molecules/cm^2 over land and 0.0-5.0×10^{15} molecules/cm^2 over the sea) and are minimum in May (5.0-10.0×10^{15} molecules/cm^2 over land and 0.0-2.0×10^{15} molecules/cm^2 over the sea). Note, the IMS scheme can exhibit a negative bias in background regions where CH_3OH concentrations are particularly low and below the detection limit of IASI, as shown by Pope et al., (2021). This bias has not been corrected for here. In 2018, $TCCH_3OH$ values are larger than in 2017 and peak in July at 12.0->15.0×10^{15} molecules/cm^2 over land and 3.0-8.0×10^{15} molecules/cm^2 over the sea) and are minimum in May at 5.0-10.0×10^{15} molecules/cm^2 over land and 1.0-5.0×10^{15} molecules/cm^2 over the sea. The $TCCH_3OH$ differences (**Figure S2 right column**) between the two years are positive over extensive areas, peaking at 5.0-10.0×10^{15} molecules/cm^2 in May over northern Europe and Scandinavia, which correlates strongly with IMS co-retrieved surface temperature differences (**Figure 1** in the main manuscript). Throughout June to August, the enhancements are lower between 2.0-5.0×10^{15} molecules/cm^2 across continental Europe.

Investigation of GOME-2 tropospheric column NO_2 ($TCNO_2$ – near-real-time level-2 product obtained from EUMETSAT at https://acsaf.org/nrt_access.php), **Figure S3**, shows peaks values over source regions of 5.0-10.0×10^{15} molecules/cm^2, which is consistent in most months and years. Background $TCNO_2$ ranges between 0.0 and 2.0×10^{15} molecules/cm^2. Between 2017 and 2018, there are enhancements over extensive areas; 1.0-3.0×10^{15} molecules/cm^2 in May and July over central Europe. Total column CO (TCCO) retrieved by IMS (**Figure S4**) peaks in May ranging between 57.0-63.0 DU over the ocean and typically 55.0-60.0 DU over continental Europe. In June and July, there is a decrease in TCCO with values ranging between 52.0 DU and 57.0 DU over the ocean and 50.0 DU to 55.0 DU over land. In August, there is an increase in TCCO with ocean values between 58.0 DU to 62.0 DU in 2017 and a peak to 65.0 DU in 2018. Over continental Europe, TCCO ranges between 45.0 DU and 60.0 in 2017 and 50.0 to 63.0 DU in 2018. In May and June, the difference panels (**right column of Figure S4**) show broad enhancements to TCCO in 2018 of 2.0 to 6.0 DU. In July, there is little difference between 2017 and 2018, while in August the largest 2018 TCCO enhancements are observed between 2.0 DU to 7.0 DU over most of continental Europe but with peak values (approximately 7.0-8.0 DU) over the central Mediterranean.

To summarize, examination of several ozone precursors which were retrieved together with ozone from Metop-A measurements all show enhancements over Europe in the summer of 2018 compared to 2017. CH_3OH is directly influenced by the observed surface temperature enhancements correlated with biogenic activity and emissions. NO_2 enhancements are generally small in scale with the largest contained to central Europe in May and July, while CO appears to be broadly enhanced across the domain in most of the summer months. While there is observational evidence of enhancements to precursor gases, and hence potentially O_3, we need to use a detailed atmospheric chemistry transport model (TOMCAT in this study) to investigate the scale of the O_3 enhancements and the processes involved.

SM 3 – Total Column Ozone

The differences in total column O_3 (TCO_3) between 2017 and 2018 for GOME-2 and IMS retrievals are shown in **Figures S5** and **S6**, respectively, and are consistent. In June, July and August, both instruments show positive differences of approximately 5.0-20.0 DU across continental Europe. In July and August (and June to a lesser extent), there are negative differences (-30.0 to -10.0 DU) across the UK, North Sea and Scandinavia. In May, there appears to be an East-West positive-negative dipole in TCO_3 across Europe. Several of the spatial features in the TCO_3 2018-2017 difference plots are consistent with the differences in SCO_3 (i.e. **Figures 3** and **4** in the main manuscript). For instance, in June (May), there are negative (positive) TCO_3 differences of <-30.0 DU (>50.0 DU) between the UK and Iceland with corresponding negative (positive) SCO_3 differences of -5.0 to 0.0 DU (2.0-5.0 DU). For GOME-2, the SCO_3 and TCO_3 spatial differences are positively correlated with values in May, June, July and August of 0.56, 0.59, 0.58 and 0.57, respectively. For IMS, the corresponding correlations in May, June, July and August were 0.60, 0.65, 0.29 and 0.54.

SM 4 – TOMCAT Biogenic Emissions

As shown by IMS retrieved surface temperature data (**Figure 1** of the main manuscript), there were substantial enhancements in May and July between 2017 and 2018 (i.e. enhancements of 3.0-8.0 K over central continental Europe and >10.0 K over Scandinavia). Higher surface temperature can increase emissions of precursor biogenic gases. Higher air temperatures can also promote chemical formation of O_3 and summer-time heat-waves are often associated with blocking events leading to atmospheric stability favourable for O_3 formation e.g. Pope et al., (2016). The latter two are accounted for automatically in TOMCAT given its detailed tropospheric chemistry scheme and prescribed reanalysis meteorological fields. However, the increase in biogenic emissions resulting from surface temperature enhancements is not represented in the standard climatological biogenic volatile organic (BVOC) emissions from the Chemistry-Climate Model Initiative (CCMI) used in TOMCAT (see Pope et al., (2020)). Therefore, we have used BVOC emissions for acetone, methanol, isoprene and monoterpenes from Jules (the Joint UK Land Environment Simulator) land surface model (Pacifico et al., 2011; Best et al., 2011; Clark et al., 2011) provided by the Centre for Ecology and Hydrology (CEH). Jules meteorological inputs came from ECMWF ERA-Interim, as for TOMCAT, the model setup used 9 plant function types and was driven by the TRIFFID global vegetation model (Zhang et al., 2015). However, the other BVOC emissions (e.g. formaldehyde, HCHO) came from CCMI as used in Pope et al., (2O20).

Figure S7 shows the combined TOMCAT input emissions (in $\mu g/m^2/s$ of C) from Jules for acetone, methanol, isoprene and monoterpenes in 2017 and 2018. In 2017, between May and August, the peak emissions are over central and eastern Europe ranging between approximately 0.35 and >0.5 $\mu g/m^2/s$. Over Scandinavia, the BVOC emissions peak in July between approximately 0.3 and 0.4 $\mu g/m^2/s$. Between 2017 and 2018, the BVOC emissions have similar rates except for Scandinavia where the emissions are >0.4 $\mu g/m^2/s$ over a larger area. The difference panels (**Figure S7 right column**) show that broadly across Europe between May and August, the BVOC emissions are larger by 0.0-0.1 $\mu g/m^2/s$ in 2018. In June, around the Alps and parts of eastern Europe, there are negative differences of -0.1 $\mu g/m^2/s$ to -0.05 $\mu g/m^2/$ due to larger 2017 BVOC emissions. The largest differences therefore are over Scandinavia, especially May and July (and June to lesser extent), where the BVOC emissions are larger by 0.2 $\mu g/m^2/s$ to >0.25 $\mu g/m^2/s$. This matches the spatial pattern in inter-year differences in $TCCH_3OH$ (**Figure S2**) retrieved by IMS providing confidence in the spatial distribution of the BVOC emissions.

It should be noted though that the annual global emission total for Jules was lower than expected (i.e. 284.0 Tg of C in 2017) when compared with CCMI isoprene emissions (461.0 Tg of C). Therefore, we decided to scale up Jules isoprene emissions in 2017 and 2018 by the same factor. As we were interested in Europe, a relatively small area of the globe, we performed the scaling in 60° longitude and latitude bins to retain more accurate regional budgets than just scaling everything uniformly globally. For consistency, though the annual totals were more comparable for the other species, the same methodology was applied to acetone, methanol and monoterpenes as well.

SM 5 – TOMCAT Evaluation

To evaluate the ability of TOMCAT to simulate the observed tropospheric O_3 behaviour, we used the GOME-2 and IMS satellite datasets and the EMEP surface sites. **Figure S8a & b** shows that over Europe, TOMCAT is able to reproduce the broad surface O_3 enhancement seen in May-June-July-August (MJJA) 2018 when compared with 2017. The EMEP sites show positive differences between 2.0 ppbv and >10.0 ppbv across Europe, peaking over central Europe with the smallest enhancements at the higher European latitudes (e.g. Scotland & Scandinavia). In comparison, TOMCAT is able to simulate the spatial pattern of the MJJA 2018 surface O_3 enhancement, but the magnitude of the difference is smaller between 1.0 ppbv and 5.0 ppbv. Over eastern Europe though, TOMCAT simulates near-zero differences whereas EMEP shows enhancements between 2.0 ppbv and 5.0 ppbv. The modelled enhancements are potentially lower than that in EMEP due, in part, to the moderate overestimation of TOMCAT surface ozone in July and August in 2017. A similar relationship is found between TOMCAT and the satellite observations, discussed later. In terms of the absolute magnitude, TOMCAT does a reasonable job reproducing the seasonal cycle and monthly mean surface O_3 values over Europe in 2017 and 2018 (i.e. TOMCAT grid boxes are co-located to EMEP sites and then used to derive the seasonal cycles – **Figures S8c** & **d**). In 2017, EMEP surface O_3 peaks at approximately 36.0-38.0 ppbv in April and May. However, TOMCAT, while simulating similar peak values, peaks several months later in May/June, and the subsequent drop off in values is less pronounced in the observations. In all months, except for December 2017, TOMCAT and EMEP monthly ranges (mean ± standard deviation) overlap showing that the model can simulate surface O_3 values observed by EMEP. Overall, the two seasonal cycles are reasonably well correlated (0.80) and the mean bias is low (-1.2 ppbv) and sits within the observational error (i.e. standard error with the autocorrelation accounted for of 3.79 ppbv). The RMSE is 3.84 ppbv and sits just outside the uncertainty range. In 2018, the model simulations only go until September and in the summer the model captures the absolute values and evolution of the observational seasonal cycle. However, in the winter and spring months, the model underestimates by 5.0-10.0 ppbv (similar in 2017 but lower differences of 0.0-5.0 ppbv). The correlation is 0.98 and both the mean bias and RMSE sit within the observational uncertainty. Therefore, TOMCAT simulates the absolute values and seasonality of the surface observations reasonably well and, although simulating smaller absolute 2018 enhancement, successfully captures the spatial distribution.

Given the relatively coarse resolution of TOMCAT, we compared the TOMCAT summer (1st May – 31st August 2018) simulation with higher resolution model data of surface ozone from the Copernicus Atmosphere Monitoring Service (CAMS). This involved two CAMS products including the global reanalysis product (available from https://ads.atmosphere.copernicus.eu/ and described by Wagner et al., (2021)) and the regional CAMS product for Europe (available from https://atmosphere.copernicus.eu/regional-services). Note, we used the ensemble reanalysis product which was an ensemble average of all the regional models involved in the CAMS regional programme. Here, CAMS global and CAMS regional had original spatial resolutions of 0.75°×0.75° and 0.1°×0.1° and were interpolated onto the TOMCAT spatial resolution for statistical comparison.

Figure S9a-c shows the summer-time average spatial surface ozone distribution over Europe for TOMCAT and both CAMS data sets. For all three models, there is peak surface ozone in the Mediterranean (~50.0-60.0 ppbv), moderate ozone levels over continental Europe (~30.0-50.0 ppbv) and lower ozone over Scandinavia (~25.0-35.0 ppbv). Here, the largest discrepancy occurs where TOMCAT has minimum surface ozone values of 25.0 ppbv while 30.0-35.0 ppbv for CAMS. However, there is generally no consistent systematic difference between TOMCAT and the CAMS datasets. For instance, there is better agreement (spatially and in absolute terms) between CAMS global and TOMCAT over the Mediterranean than CAMS regional, while the opposite is true for CAMS regional and TOMCAT in central Europe. TOMCAT surface ozone has a good spatial correlation with CAMS global (R=0.66) and CAMS regional (R=0.76) surface ozone. The percentage root-mean-square-error (RMSE%) between CAMS global and CAMS regional with TOMCAT is 16.8% and 14.5%, respectively. Comparisons of CAMS global and CAMS regional yield metrics of R=0.77 and RMSE%=12.5%. Therefore, the spatial domain metrics between all three data sets are consistent suggesting TOMCAT surface ozone is consistent with that of these higher resolution models.

Figure S9d shows the daily domain average time-series of the three data sets. TOMCAT typically simulates summer-time surface ozone values between that of CAMS global and CAMS regional (apart from the first half of May where it has a low bias of 3.0-5.0 ppbv). The median and 25th-75th percentile values of the time-series are also shown. The median values are very similar at 38.1, 39.4 and 37.9 ppbv for TOMCAT, CAMS global and CAMS regional, respectively. The 25th-75th percentiles have similar surface ozone values, but the TOMCAT inter-quartile range (IQR) is slightly smaller (1.6 ppbv) than CAMS global (3.2 ppbv) and CAMS regional (5.1 ppbv). The time-series R (RMSE%) values between TOMCAT and CAMS global and CAMS regional are 0.76 (6.4%) and 0.75 (4.7%), respectively. The inter-CAMS R and RMSE% are 0.9 and 6.8%. Therefore, TOMCAT successfully reproduces the summer 2018 surface ozone values over Europe in comparison to higher resolution model datasets, which have assimilated observations. Thus, providing further confidence in TOMCAT simulated ozone.

There is good consistency between GOME-2 (**Figure S10**) and IMS retrieved SCO_3 (**Figure S12**), both showing substantial SCO_3 enhancements (4.0-8.0 DU for GOME-2 and 3.0-6.0 DU for IMS) in May and July over continental Europe. In June and August, both GOME-2 and IASI show smaller scale SCO_3 enhancements of 1.0-3.5 DU across Europe. In April and May, both instruments show enhancements over the North Atlantic (3.0-9.0 DU). The spatial correlation between instruments over Europe (i.e. domain in **Figures S10-13**) ranges between 0.21 and 0.47 for the monthly differences. Therefore, considering that the GOME-2 and IASI retrievals use ultraviolet (UV) and infrared (IR) wavelengths, respectively, with peak vertical sensitivities in the lower and mid/upper troposphere, consistency in the magnitudes and patterns of the 2018-2017 enhancements in retrieved SCO_3 indicates these to extend over the bulk of the troposphere. It also provides confidence in these satellite observations to detect regional tropospheric spatiotemporal variability. To evaluate TOMCAT and assess its ability to simulate enhancements in SCO_3 in comparison to GOME-2 and IASI, the satellite averaging kernels (AKs) (i.e. the satellite vertical smearing) need to be applied to TOMCAT to allow for like-for-like comparisons. The GOME-2 (**Equation S1**) and IASI (**Equation S2**) AKs are applied as:

$$\boldsymbol{TOMCAT_{AK} = AK.TOMCAT_{int} + imak\_sc\_apr} \qquad \text{(S1)}$$

$$\boldsymbol{TOMCAT_{AK} = AK.(TOMCAT_{int} - apr) + apr} \qquad \text{(S2)}$$

where $\boldsymbol{TOMCAT_{AK}}$ is the modified model sub-column profile (DU), ***AK*** is the averaging kernel matrix, $\boldsymbol{TOMCAT_{int}}$ is the TOMCAT sub-column profile (DU) on the satellite pressure grid and ***apr*** is the apriori (DU) and ***imak_sc_apr*** represents the term ***(I-AK).apr*** where ***I*** is the identity matrix.

For TOMCAT with GOME-2 or IMS AKs applied in **Figures S11** and **S13**, positive SCO_3 differences occur primarily in May and July (1.0-3.0 DU) over continental Europe, similarly to the respective retrievals. In June and August, again like the respective retrievals, the SCO_3 enhancements over Europe are widespread but weaker between 0.0 to 2.0 DU (though more noticeable in TOMCAT_IASI_AK). Also, in April and May, both TOMCAT data sets show SCO_3 enhancements over the North Atlantic (0.0-2.0 DU for TOMCAT_G2_AK and 1.0-3.0 DU for TOMCAT_IASI_AK). There are a few observed instances of negative difference (e.g. -2.0 to 0.0 DU) over central Europe in September and the mid-North Atlantic in May and June. However, the TOMCAT signal tends to be weaker. In terms of spatial patterns in the SCO_3 difference between 2017 and 2018, correlations between TOMCAT_G2_AK and GOME-2 range between 0.33 and 0.54 over Europe for monthly data and 0.47 for a six monthly average. For TOMCAT_IASI_AK and IASI, they range between 0.39 and 0.63 for monthly data and 0.53 for a six monthly average.

In summary, TOMCAT is able to reproduce the sign and spatial distribution of the 2018-2017 O_3 differences in the surface and satellite observations. Through the summer months of 2018, TOMCAT, like the observations, shows there are enhancements in surface/lower tropospheric O_3 in 2018, but the absolute magnitude tends to be larger in the observational datasets. Therefore, we consider the

TOMCAT model to be a suitable tool to diagnose the drivers of the European summer 2018 lower tropospheric O_3 enhancements.

SM 6 – ROTRAJ Back-trajectories

Advection of tropospheric O_3-rich air masses into Europe potentially contributed towards the observed enhancements in the summer of 2018. To investigate this we have utilised back-trajectories from the Reading Offline Trajectory Model (ROTRAJ), a Lagrangian atmospheric transport model (Methven *et al*., 2003), to quantify the import of O_3 into the domain. ROTRAJ was initialised over Paris and Berlin (two central locations within the domain) and back-trajectories released for 10 days in 6 hour intervals (i.e. 41 points, including release point). A back-trajectory was released every 6 hours throughout May to August in 2017 and 2018 (i.e. 492 back-trajectories in total) with output at 00 UTC, 06 UTC, 12 UTC and 18 UTC. As we investigate modelled O_3 at the surface and at 500 hPa, the back-trajectories where released at these two altitudes. In total, ROTRAJ was run 8 times (i.e. 2 years x 2 locations x 2 altitudes). To determine the level of O_3 being transported into the domain, each trajectory point in the trajectory path was co-located with TOMCAT O_3 data (i.e. the closest grid box, altitude level and model 6-hourly time step) and the trajectory O_3 average determined (i.e. back-trajectories from O_3-rich air masses will be larger). These O_3-weighted back-trajectories (O_3WBT) for Paris and Berlin (May-August 2017 & 2018) at the surface and 500 hPa have been plotted in **Figures S14** and **15**. However, as the O_3WBT are subject to large scale variability, they have been averaged them onto the TOMCAT horizontal spatial resolution in the corresponding panels in **Figures S16**and **17**.

When initialised at the surface in Paris (**Figure S16a** & **b**) the O_3WBT range from 40.0 ppbv to >50.0 ppbv over continental Europe in both years, but 40.0-45.0 ppbv and 33.0-40.0 ppbv over the North Atlantic in 2017 and 2018, respectively. A similar spatial pattern occurs when initialised at the surface over Berlin (**Figure S17a** & **b**) where continental Europe has O_3WBT values of 40.0-50.0 ppbv in both years (though approximately 30.0 ppbv over Scandinavia in 2017). Over the North Atlantic, this ranges from 40.0-45.0 ppbv and 35.0-42.0 ppbv in 2017 and 2018, respectively. This appears to suggest that in 2017, the import of O_3-rich air masses into Europe was larger than that of 2018. Therefore, the surface enhancements in O_3 in the summer of 2018 were predominantly not from advected O_3 into the domain.

At approximately 500 hPa, a different relationship exists. As the back-trajectories are initialised at a higher altitude, with larger horizontal wind velocities (i.e. the free troposphere), they originate from distances further way than those at the surface. When initialised over Paris at approximately 500 hPa (**Figure S16c** & **d)**, the O_3WBT values are more spatially uniform, increasing in value towards the Arctic. Below and above 50°N, the O_3WBT values range from 45.0-60.0 ppbv and from 50.0-80.0 ppbv, respectively, in 2017. For 2018, a similar spatial pattern occurs but with larger O_3WBT values over the southern North Atlantic of 55.0-65.0 ppbv. For Berlin at approximately 500 hPa (**Figure SM6c** & **d**), the same large scale signal exists with similar absolute O_3WBT values. Therefore, there appears to be transport of O_3-rich air in 2018 (typically 3.0-7.0 ppbv larger than in 2017) from the southern North Atlantic to the 500 hPa layer over Europe helping to promote the observed and modelled summer-time 2018 enhancements. However, between approximately 50°N and 60°N, the 2017 O_3WBT values tend to be slightly larger (e.g. by 3.0-5.0 ppbv in places), which will partially offset the southern North Atlantic signal.

To investigate the vertical extent of the profiles, we plot time-pressure profiles for each year of the trajectories released at both sites and altitudes (**Figure S18-S21**). The trajectories are grouped by locations originating north and south of the release points to add some spatial context (e.g. are they from the southern North Atlantic or northern North Atlantic). When initialised from Paris at the surface (**Figure S18)**, the majority of the trajectories originated north of the release point in both 2017 and 2018. Trajectories originating south of the site have an average O_3WBT value of 41.7 ppbv and 42.1 ppbv in 2017 and 2018. Therefore, there is little difference between them and are all constrained to the troposphere (peak trajectories originate from approximately 500 hPa). For sites originating north of the release point, the sample sizes are larger with similar average O_3WBT values of 39.4 ppbv and 39.6 ppbv between years. Though, there is a larger vertical distribution in the trajectories with more originating from the mid-troposphere (600-400 hPa). When initialised from Berlin, at the surface (**Figure S19**), the trajectories originating from the south are less frequent but do show a larger flux of O_3 towards the release site in 2017 than 2018 with O_3WBT values of 40.7 ppbv and 37.4 ppbv. North of the release point, again there are many more trajectories. Here, the vertical distribution for both years is consistent with that of Paris (**Figure S18**) and have average O_3WBT values of 39.5 ppbv and 38.3 ppbv. Therefore, this is generally supportive that advection of O_3-rich air into continental Europe was larger in the summer of 2017 than 2018.

When released at 500 hPa, for both release points, the advection of O_3-rich air was more substantial in 2018. For Paris (**Figure S20**), the average O_3WBT values, for trajectories originating south of the release point, were 57.3 ppbv and 59.8 ppbv for both years. North of the release site, this was 70.9 ppbv and 75.9 ppbv for 2017 and 2018. For Berlin (**Figure S21**), the corresponding average O_3WBT values (south of release point) were 55.0 ppbv and 59.3 ppbv in 2017 and 2018 and (north of release point) was 73.4 ppbv in both years. Vertically, for both release points and years, trajectories south of the release points range from the surface (50.0-65.0 ppbv) and 300 hPa (60.0-75.0 ppbv). North of the release points, the trajectories are more constrained to the lower troposphere (800-600 hPa with O_3WBT values of 50.0-70.0 ppbv) and upper troposphere 350-250 hPa (O_3WBT >80.0 ppbv). Here, the bulk of the trajectories, before converging on 500 hPa by Day 0, are between 400 and 250 hPa with larger O_3WBT values (70->80.0 ppbv). Therefore, trajectories originating south of the release point are representative of tropospheric O_3, while north of the release point (where the tropopause is lower in altitude) the trajectories are exposed to O_3-rich airmasses originating from the lower stratosphere (i.e. the back trajectories have close proximity to the tropopause pressure – see **Figures S20 & 21**). Overall, though, advection of O_3-rich air into continental Europe is more pronounced in 2018 over 2017 at the 500 hPa level. Based on the spatial maps (**Figures S16-S17** and **Figure 12** of the main manuscript, this 2018 O_3 enhancement is predominantly originating from tropospheric sources in the southern North Atlantic.

References

Best, M.J., Pryor, M., Clark, D.B., et al.: The Joint UK Land Environment Simulator (JULES), model description—Part 1: energy and water fluxes, *Geoscientific Model Development*, 4, 677–699, doi: 10.5194/gmd-4-677-2011, 2011.

Clark, D. B., Mercado, L.M., Sitch, S., et al.: The Joint UK Land Environment Simulator (JULES), model description—Part 2: carbon fluxes and vegetation dynamics, *Geoscientific Model Development,* 4, 701–722, doi: doi.org/10.5194/gmd-4-701-2011, 2011.

Methven, J., Arnold, S.R., O'Connor, F.M., et al.: Estimating photochemically produced ozone throughout a domain using flight data and a Lagrangian model, *Journal of Geophysical Research: Atmospheres,* **10** (D9), doi:10.1029/2002JD002955, 2003.

Pacifico, F., Harrison, S.P., Jones, C.D., et al.: Evaluation of a photosynthesis-based biogenic isoprene emission scheme in JULES and simulation of isoprene emissions under present-day climate conditions, *Atmospheric Chemistry and Physics,* 11, 4371–4389, doi**:** 10.5194/acp-11-4371-2011, 2011.

Pope, R.J., Butt, E.W., Chipperfield, M.P., et al.: The impact of synoptic weather on UK surface ozone and implications for premature mortality. *Environmental Research Letters,* **11**, 124004, doi:10.1088/1748-9326/11/12/124004, 2016.

Pope, R.J., Arnold, S.R., Chipperfield, M.P., et al.: Substantial Increases in Eastern Amazon and Cerrado Biomass Burning-Sourced Tropospheric Ozone. *Geophysical Research Letters*, 47 (3), e2019GL084143, doi: 10.1029/2019GL084143, 2020.

Pope, R. J., Kerridge, B. J., Siddans, R., et al.: Large enhancements in southern hemisphere satellite-observed trace gases due to the 2019/2020 Australian wildfires, *Journal of Geophysical Research: Atmospheres*, 1–13, doi:10.1029/2021jd034892, 2021.

Wagner, A., Bennouna, Y., Blechschmidt, A.M., et al.: Comprehensive evaluation of the Copernicus Atmosphere Monitoring Service (CAMS) reanalysis against independent observations: Reactive gases, *Elementa: Science of the Anthropocene*, 9 (1), doi: 10.1525/elementa.2020.00171., 2021.

Zhang, Z., Xue, Y., MacDonald, G., et al.: Investigation of North American vegetation variability under recent climate: A study using the SSiB4/TRIFFID biophysical/dynamic vegetation model, *Journal of Geophysical Research: Atmospheres*, 120: 1300– 1321. doi: 10.1002/2014JD021963, 2015.

Figures:

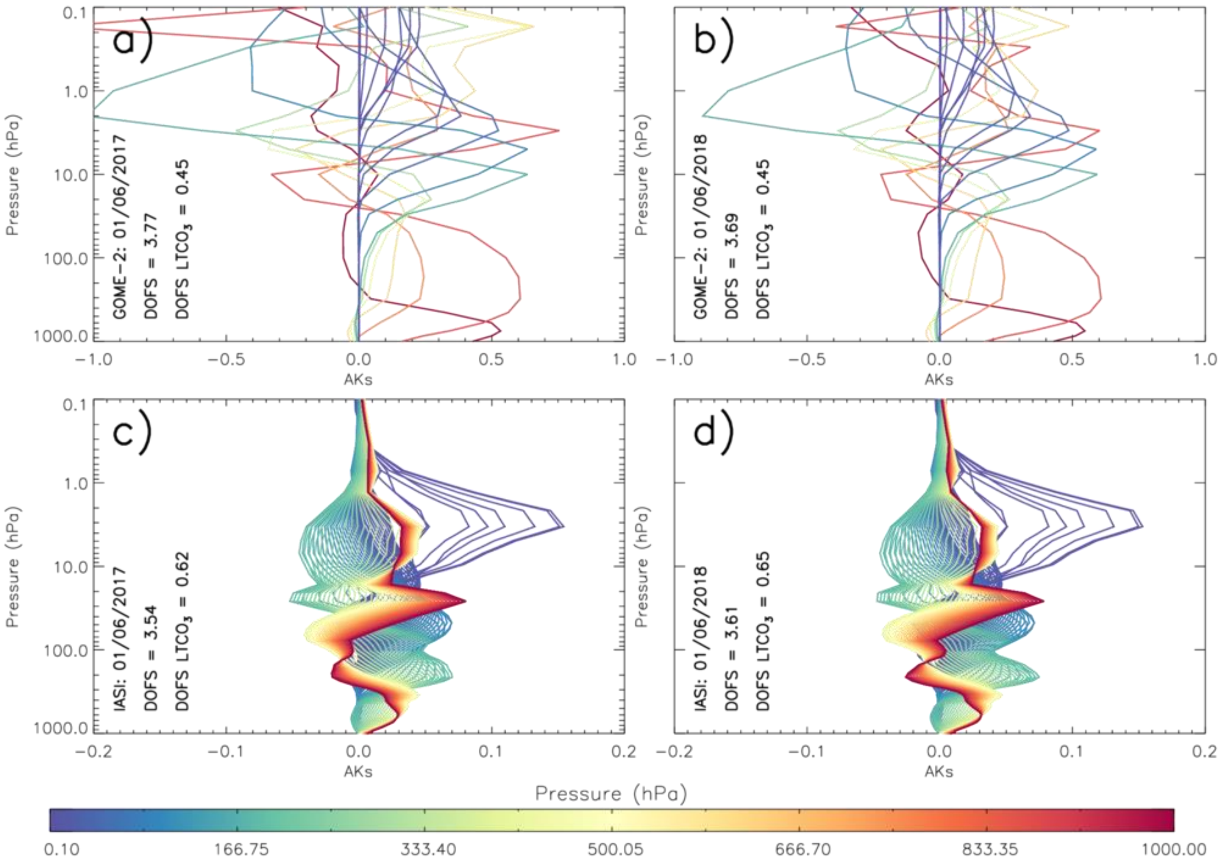

Figure S1: Example European domain average averaging kernels (AKs) for retrieved ozone profiles for a) GOME-2 on the 1st June 2017, b) GOME-2 on the 1st June 2018, c) IMS on the 1st June 2017 and d) IMS on the 1st June 2018. The degrees of freedom of signal (DOFS) for the full profile and lowest sub-column ($LTCO_3$, surface – 450 hPa) are also shown.

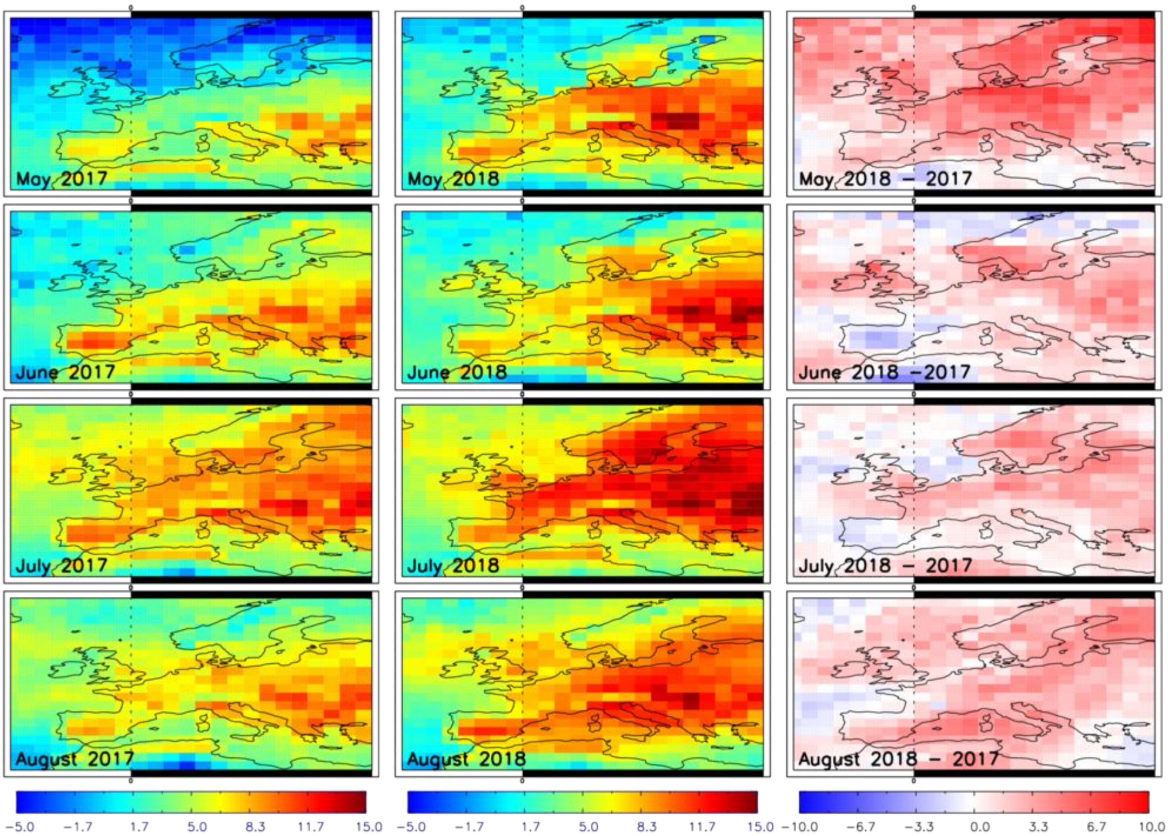

Figure S2: *Total column methanol retrieved from Metop-A by the extended IMS scheme (CH_3OH, $\times 10^{15}$molecules/cm^2) for May to August in 2017 (left column), 2018 (centre column) and 2018-2017 difference (right column) over Europe.*

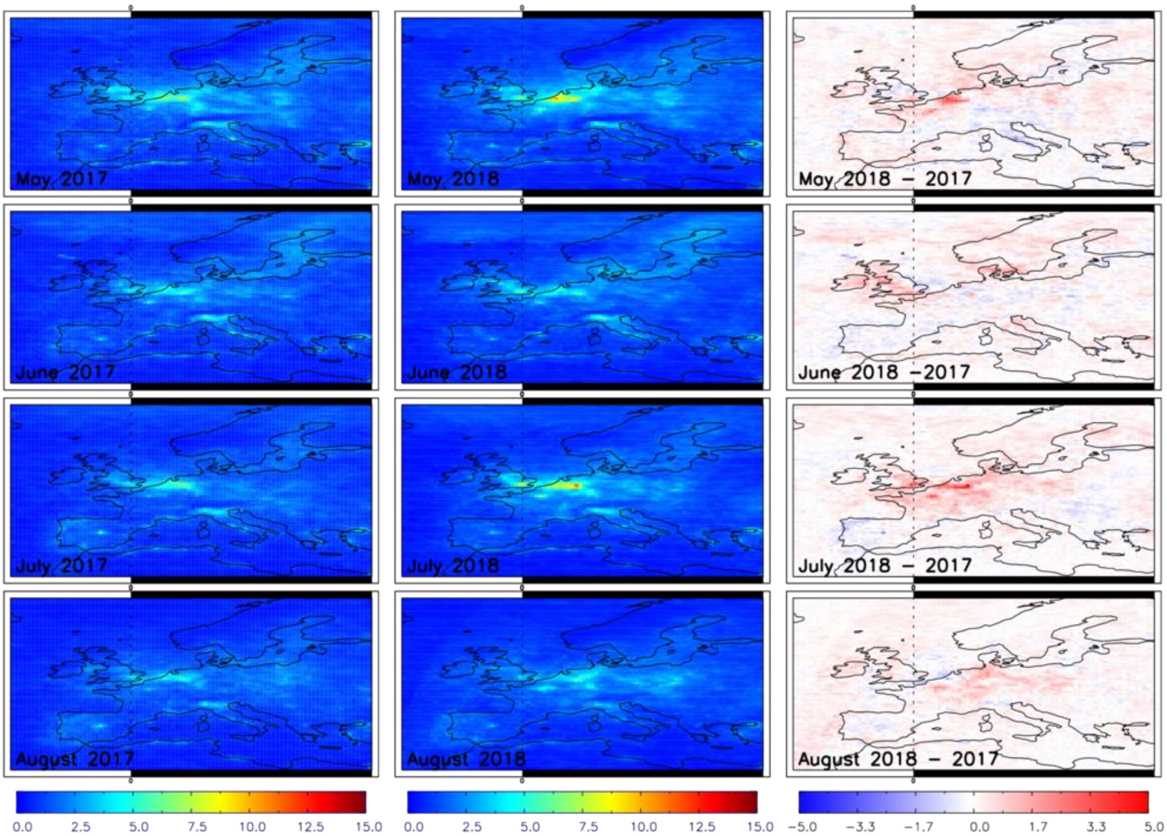

Figure S3: *GOME-2 tropospheric column nitrogen dioxide (NO_2, $\times10^{15}$molecules/cm^2) for May to August in 2017 (left column), 2018 (centre column) and 2018-2017 difference (right column) over Europe.*

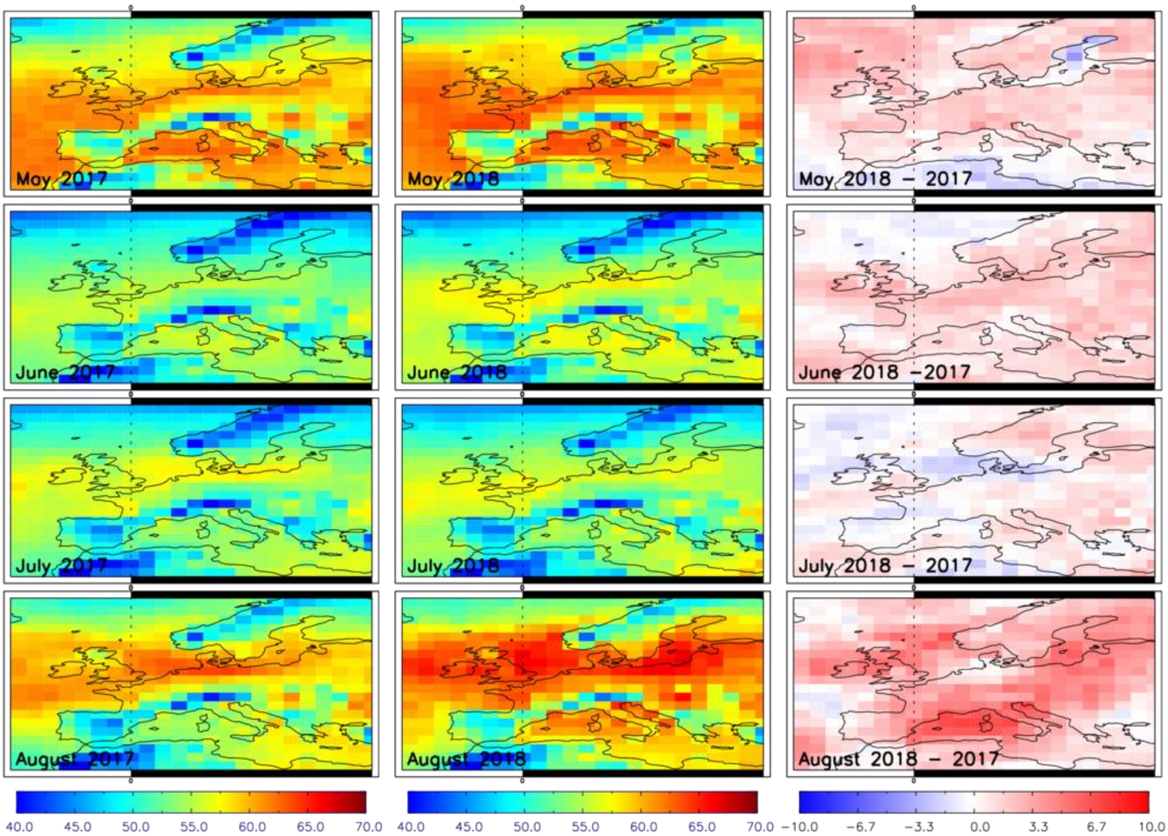

Figure S4: *Total column carbon monoxide retrieved from MetOp-A by the extended IMS scheme (CO, Dobson units (DU)) for May to August in 2017 (left column), 2018 (centre column) and 2018-2017 difference (right column) over Europe.*

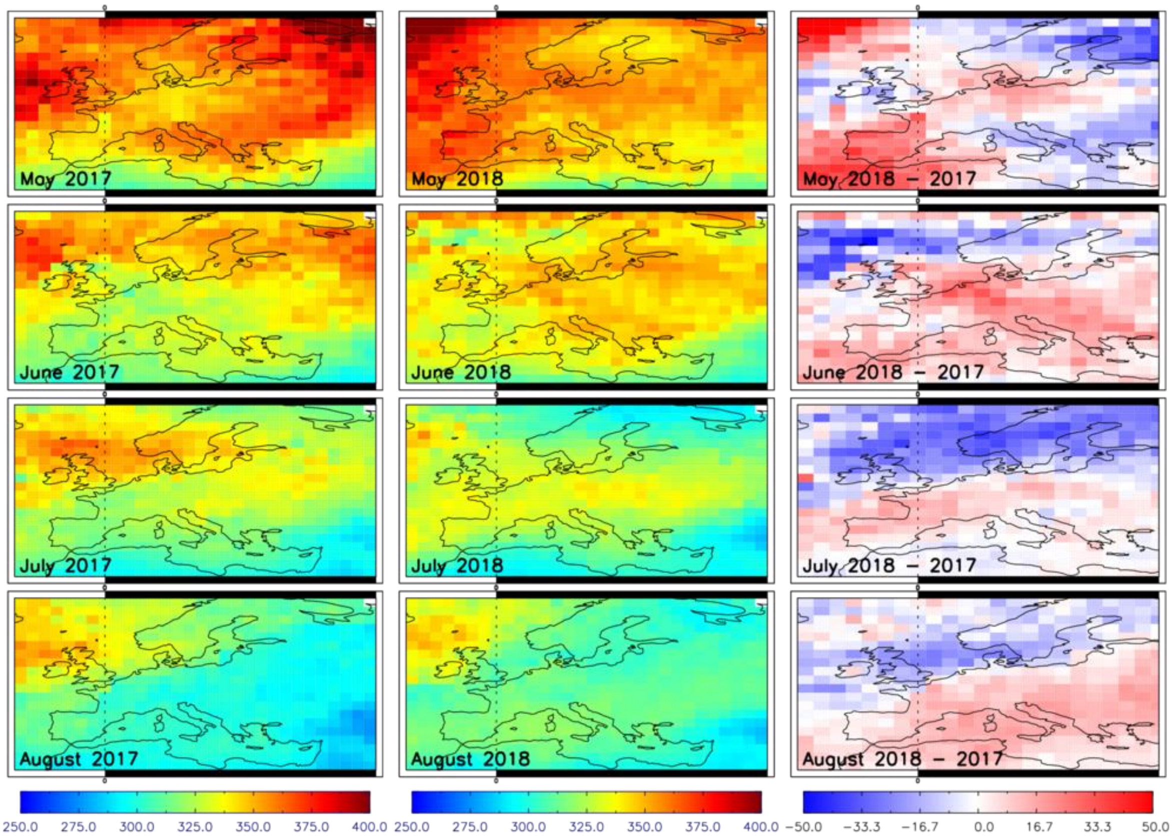

Figure S5: *GOME-2 total column ozone (O_3, DU) for May to August in 2017 (left column), 2018 (centre column) and 2018-2017 difference (right column) over Europe.*

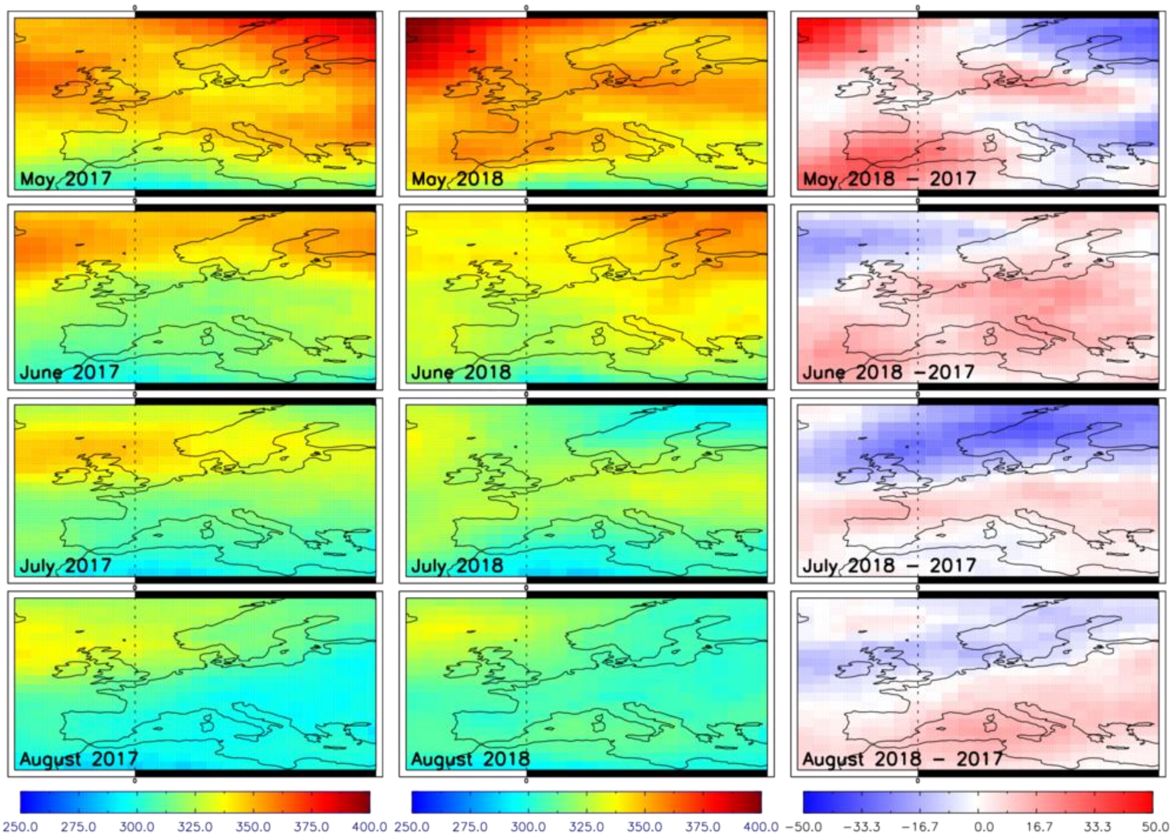

Figure S6: *Total column O_3 (DU) retrieved from MetOp-A by the extended IMS scheme for May to August in 2017 (left column), 2018 (centre column) and 2018-2017 difference (right column) over Europe.*

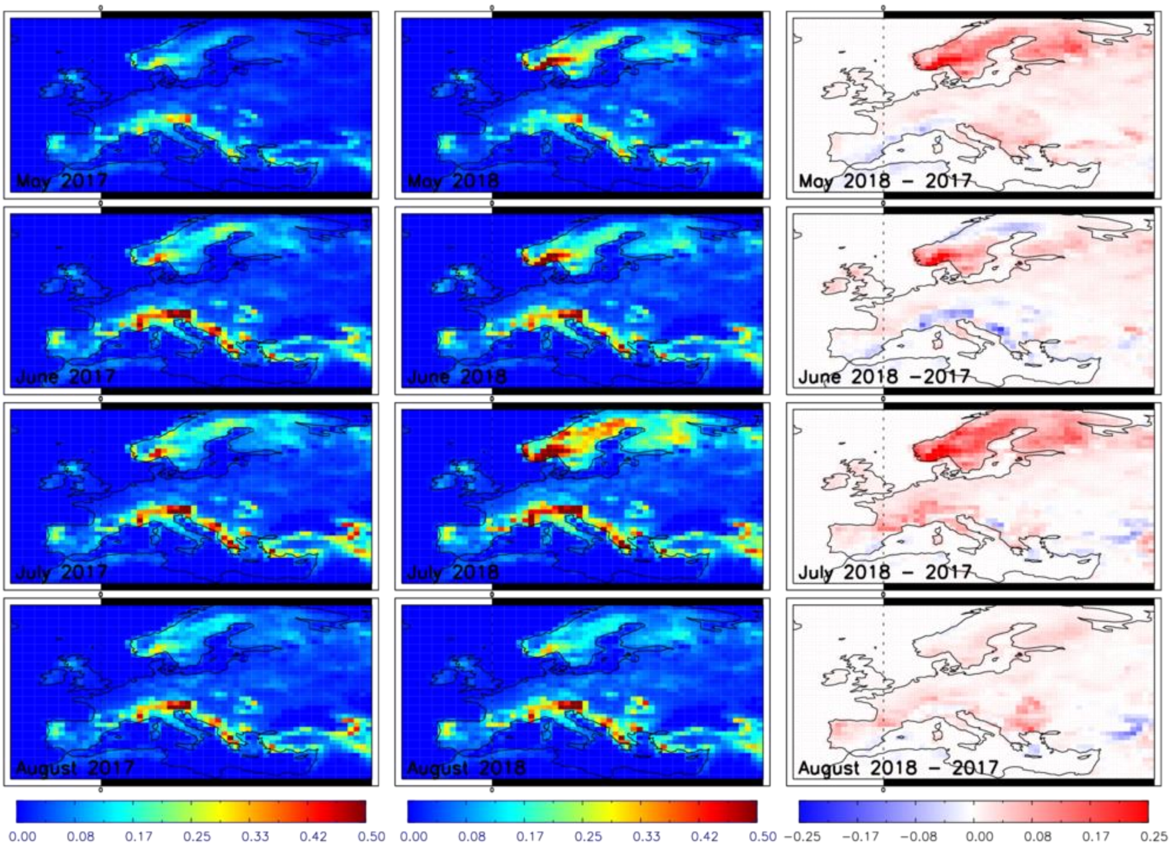

Figure S7: *JULES biogenic emissions (summation of isoprene, acetone, methanol and monoterpenes in µg/m^2/s of C) for May to August in 2017 (left column), 2018 (centre column) and 2018-2017 difference (right column) over Europe.*

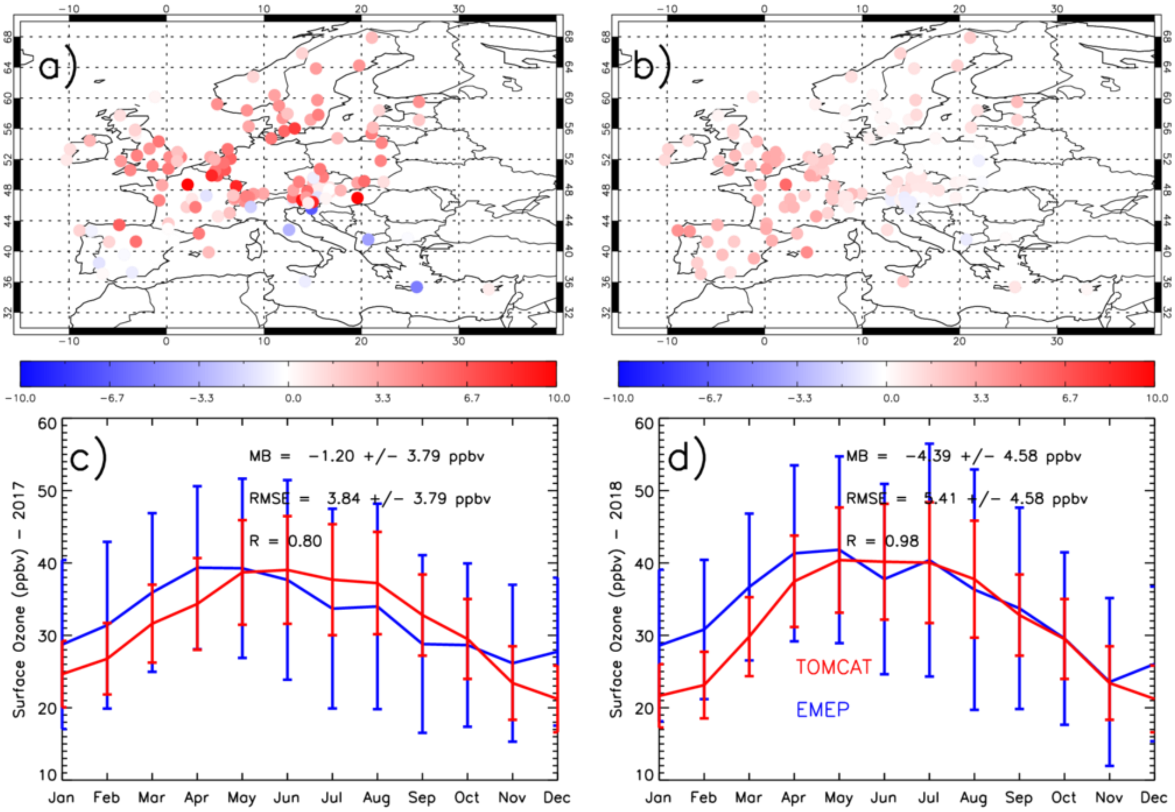

Figure S8: *Surface O_3 (ppbv) May-June-July-August 2018-2017 average difference for a) EMEP sites and b) TOMCAT. The observational (blue) and modelled (red) surface O_3 seasonal cycle are for c) 2017 and d) 2018. Vertical bars represent the monthly standard deviations. The statistics in the top right of c) and d) are the mean bias (MB), the root mean square error (RMSE) and correlation (R). The uncertainties on the MB and RMSE are the standard errors corrected for temporal autocorrelation.*

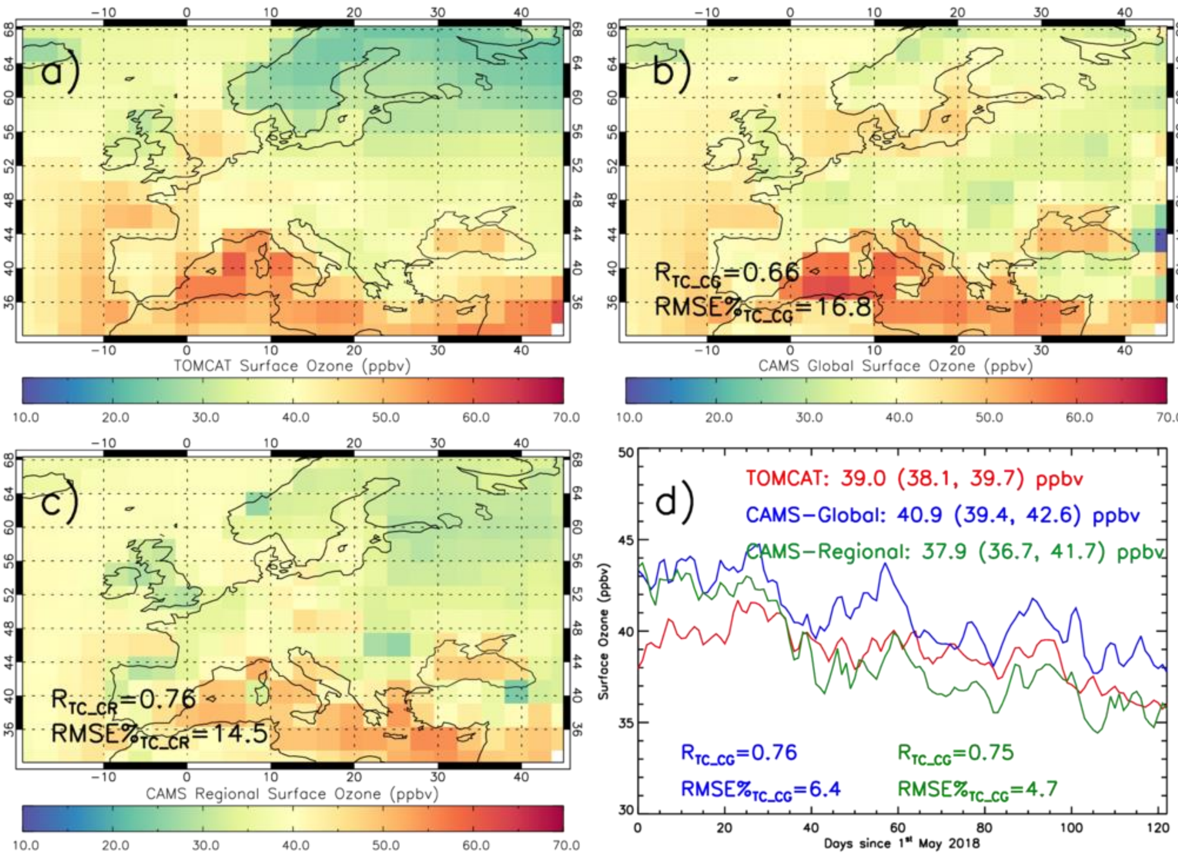

Figure S9: Surface ozone (ppbv) averaged between 1st May and 31st August 2018 for a) TOMCAT, b) CAMS global reanalyses and c) CAMS regional reanalyses. The correlation (R) and percentage root-mean-square-error (RMSE%) between TOMCAT and CAMS global (CG) and CAMS regional (CR) reanalyses are shown in the bottom of panels b) and c). Panel d) shows the daily domain average surface ozone (ppbv) time-series between 1st May and 31st August 2018 for TOMCAT (red), CAMS global reanalyses (blue) and CAMS regional reanalyses (green). The number after the model labels are the time-series median (25th percentile, 75th percentile) values. The R and RMSE% metrics show the same information as the maps but between the TOMCAT and CAMS time-series (coloured accordingly).

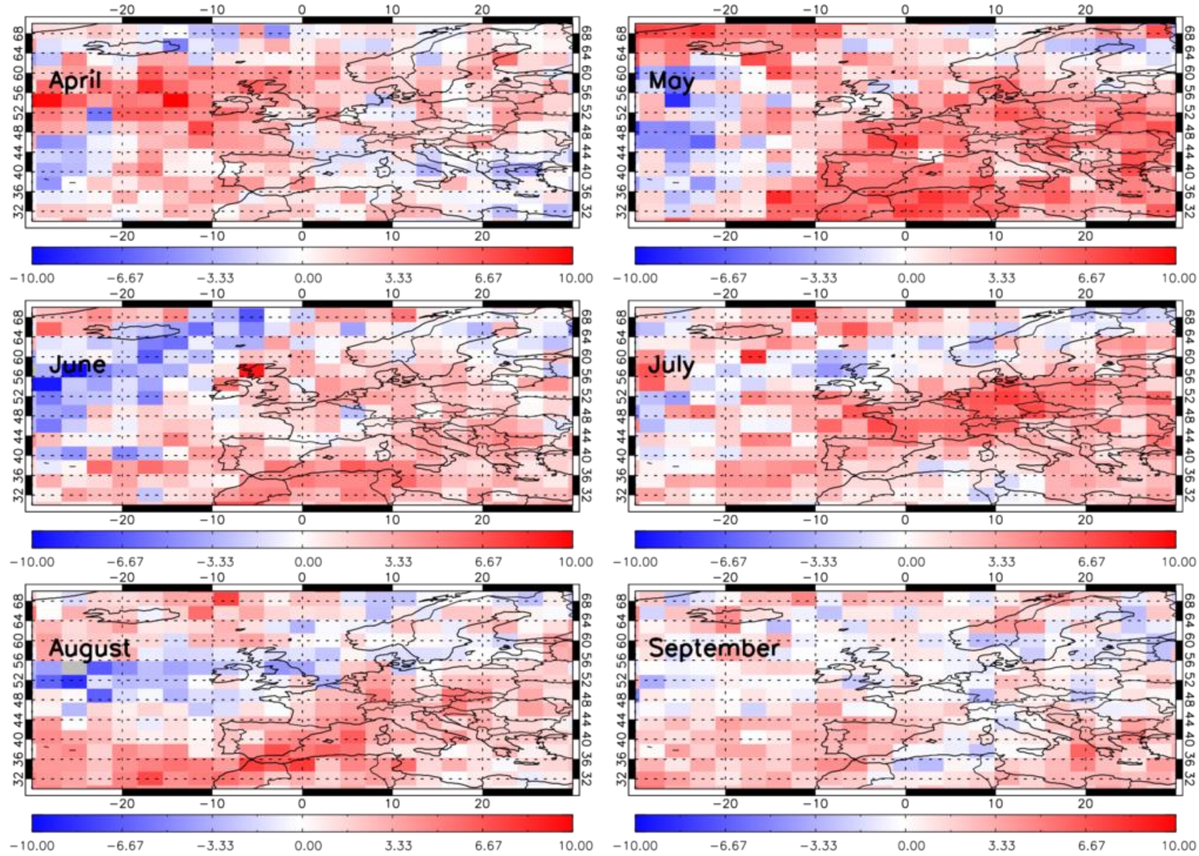

Figure S10: *Surface-450hPa sub-column ozone (SCO_3) 2018-2017 differences from GOME-2 for April to September over Europe. SCO_3 units are in Dobson units (DU).*

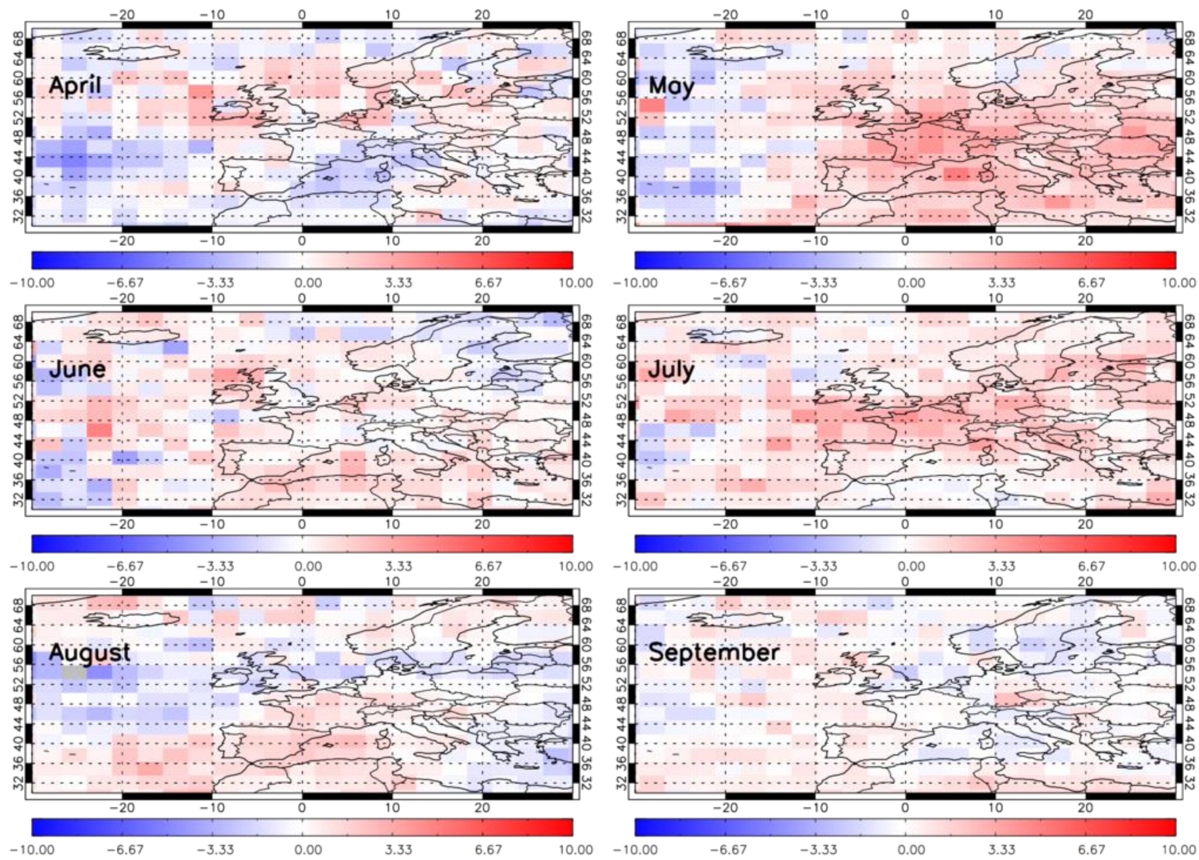

Figure S11: *Surface-450hPa TOMCAT SCO_3 (DU), with the GOME-2 averaging kernels (AKs) applied, 2018-2017 differences for April to September over Europe.*

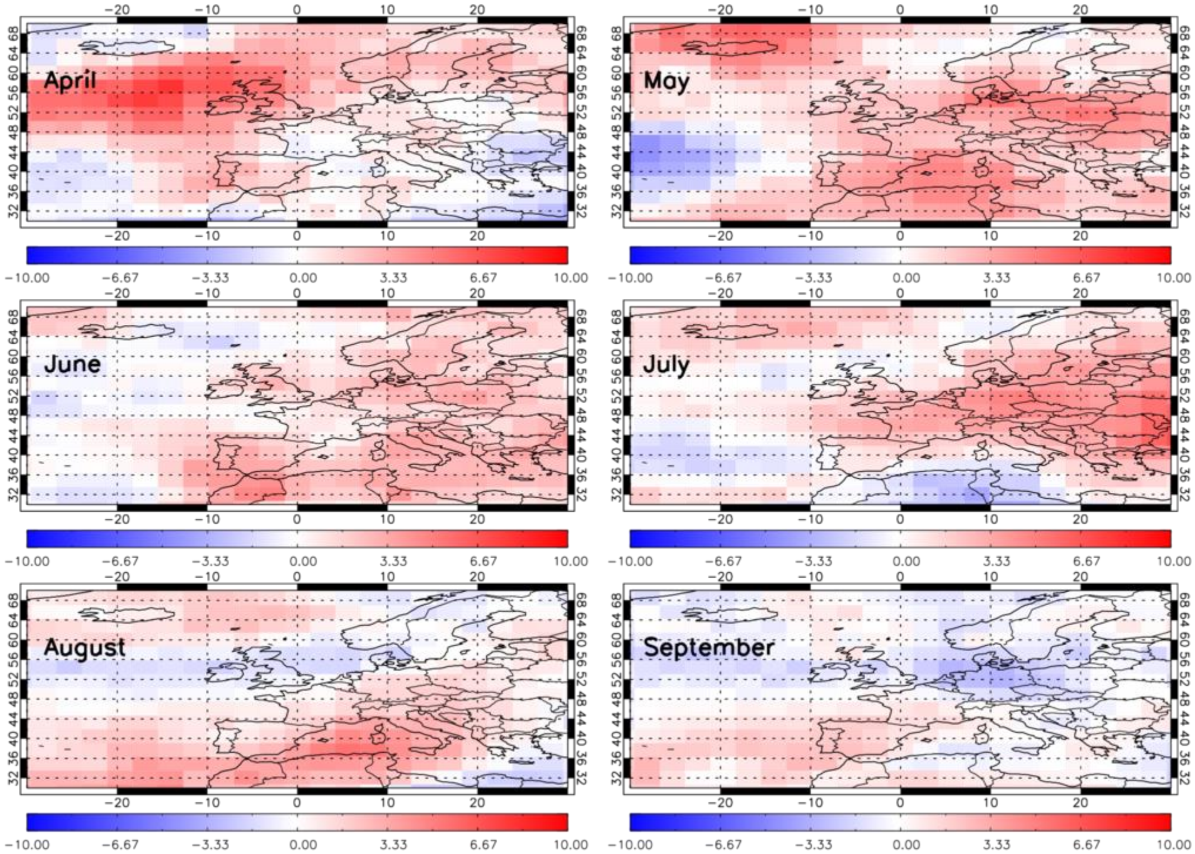

Figure S12: *Surface-450hPa IMS SCO_3 (DU) 2018-2017 differences for April to September over Europe.*

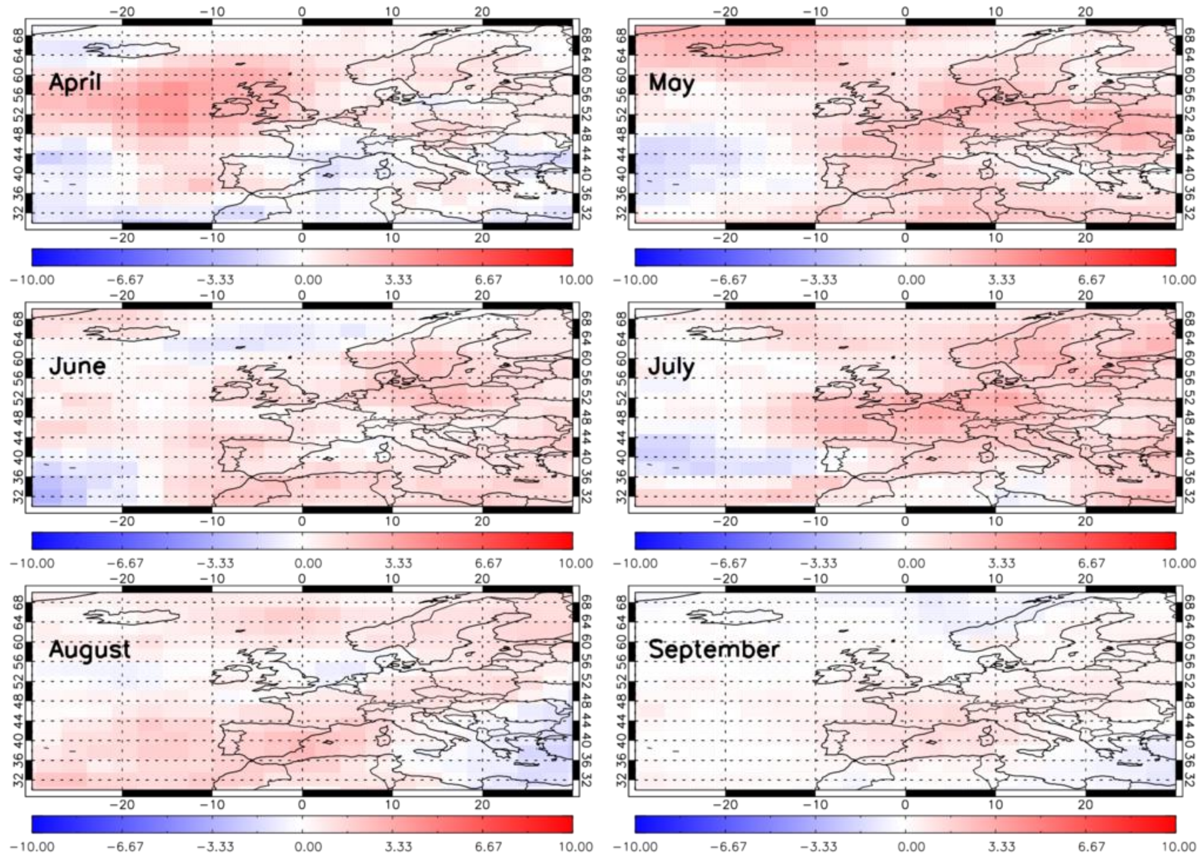

Figure S13: *Surface-450hPa TOMCAT SCO_3 (DU), with the IMS averaging kernels (AKs) applied, 2018-2017 differences for April to September over Europe.*

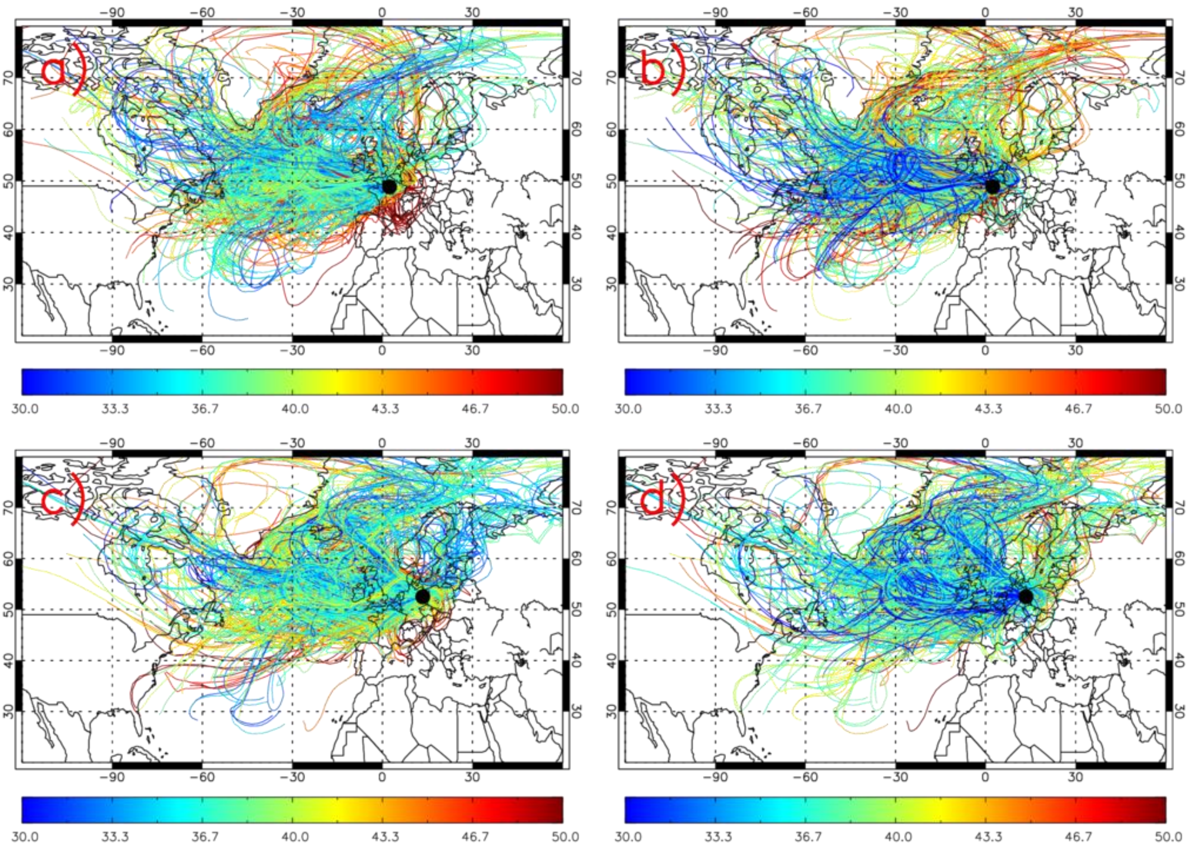

Figure S14: *ROTRAJ back-trajectories (10 days), weighted by the average TOMCAT* O_3 *(ppbv) concentration along each trajectory path, for a) Paris at the surface between May and August in 2017, b) Paris at the surface between May and August in 2018, c) Berlin at the surface between May and August in 2017 and d) Berlin at the surface between May and August in 2018. The black circles represent the location of Paris and Berlin where the trajectories were released from.*

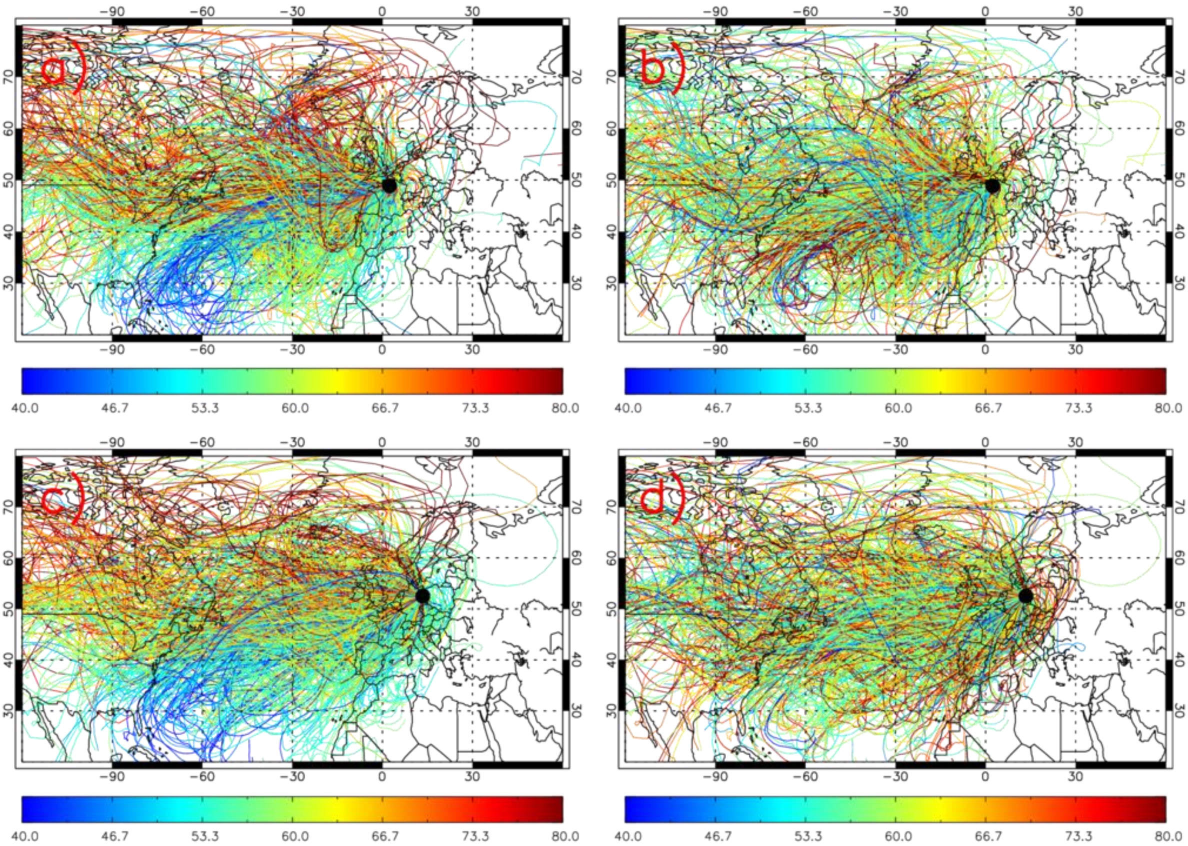

Figure S15: *ROTRAJ back-trajectories (10 days), weighted by the average TOMCAT* O_3 *(ppbv) concentration along each trajectory path, for a) Paris at approximately 500 hPa between May and August in 2017, b) Paris at approximately 500 hPa between May and August in 2018, c) Berlin at approximately 500 hPa between May and August in 2017 and d) Berlin at approximately 500 hPa between May and August in 2018. The black circles represent the location of Paris and Berlin where the trajectories were released from.*

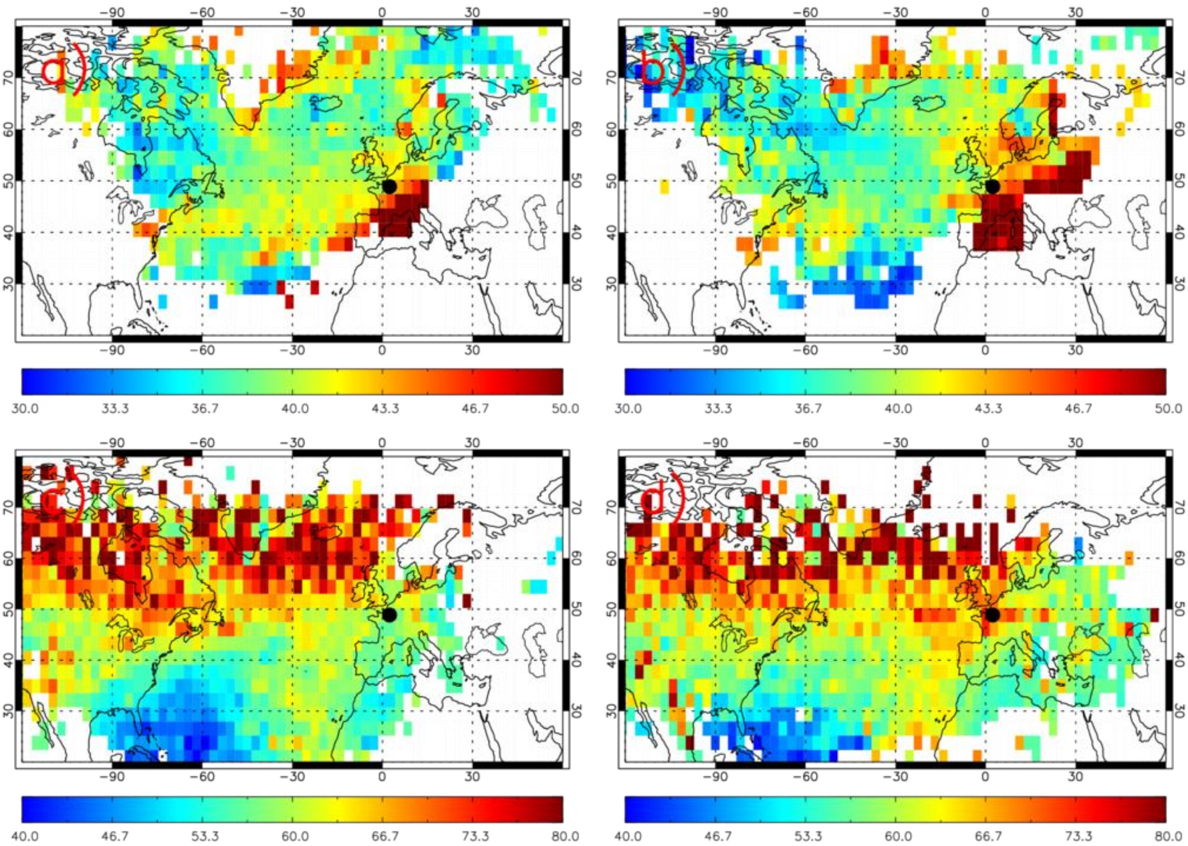

Figure S16: *ROTRAJ back-trajectories (10 days) released from Paris (May-August), weighted by the average TOMCAT O_3 (ppbv) concentration along each trajectory path, gridded onto the TOMCAT horizontal resolution for a) at the surface in 2017, b) at the surface in 2018, c) at approximately 500 hPa in 2017 and d) at approximately 500 hPa in 2018. The black circles represent the location of Paris where the trajectories were released from.*

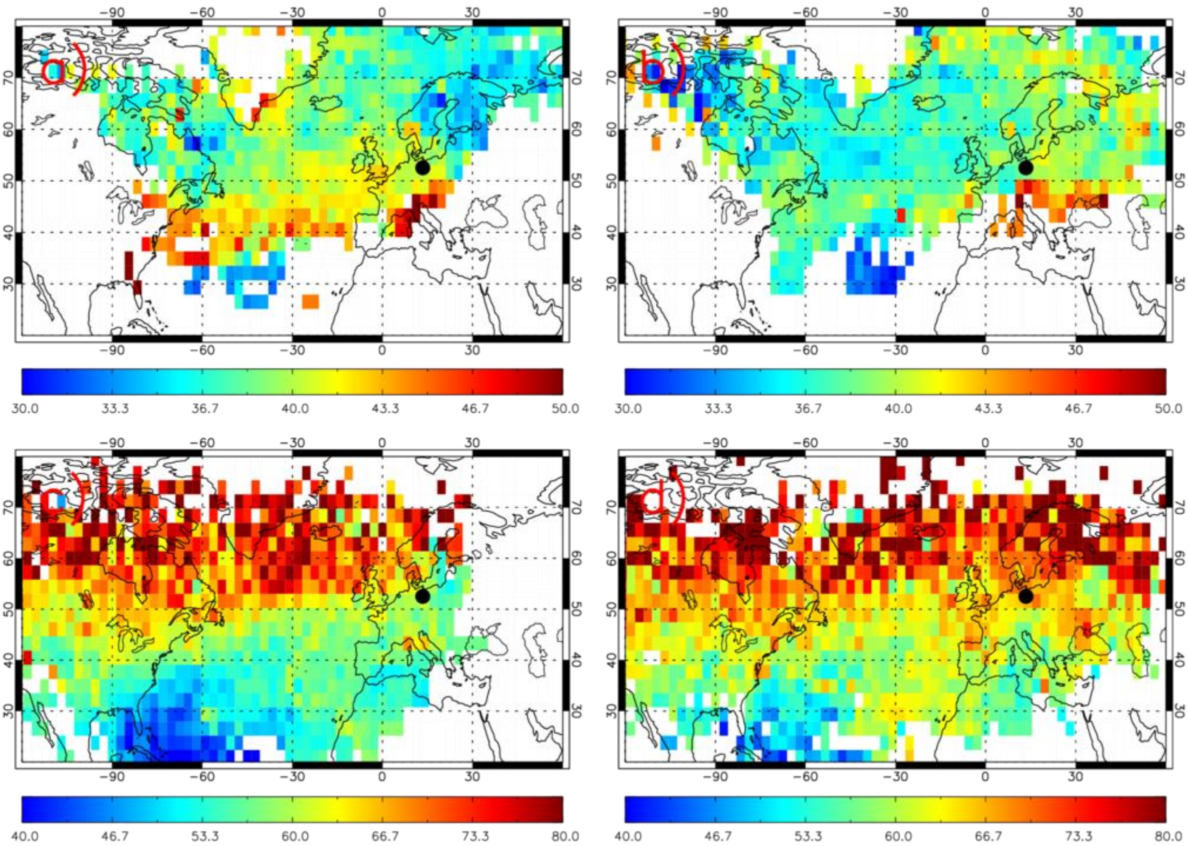

Figure S17*: ROTRAJ back-trajectories (10 days) released from Berlin (May-August), weighted by the average TOMCAT O_3 (ppbv) concentration along each trajectory path, gridded onto the TOMCAT horizontal resolution for a) at the surface in 2017, b) at the surface in 2018, c) at approximately 500 hPa in 2017 and d) at approximately 500 hPa in 2018. The black circles represent the location of Berlin where the trajectories were released from.*

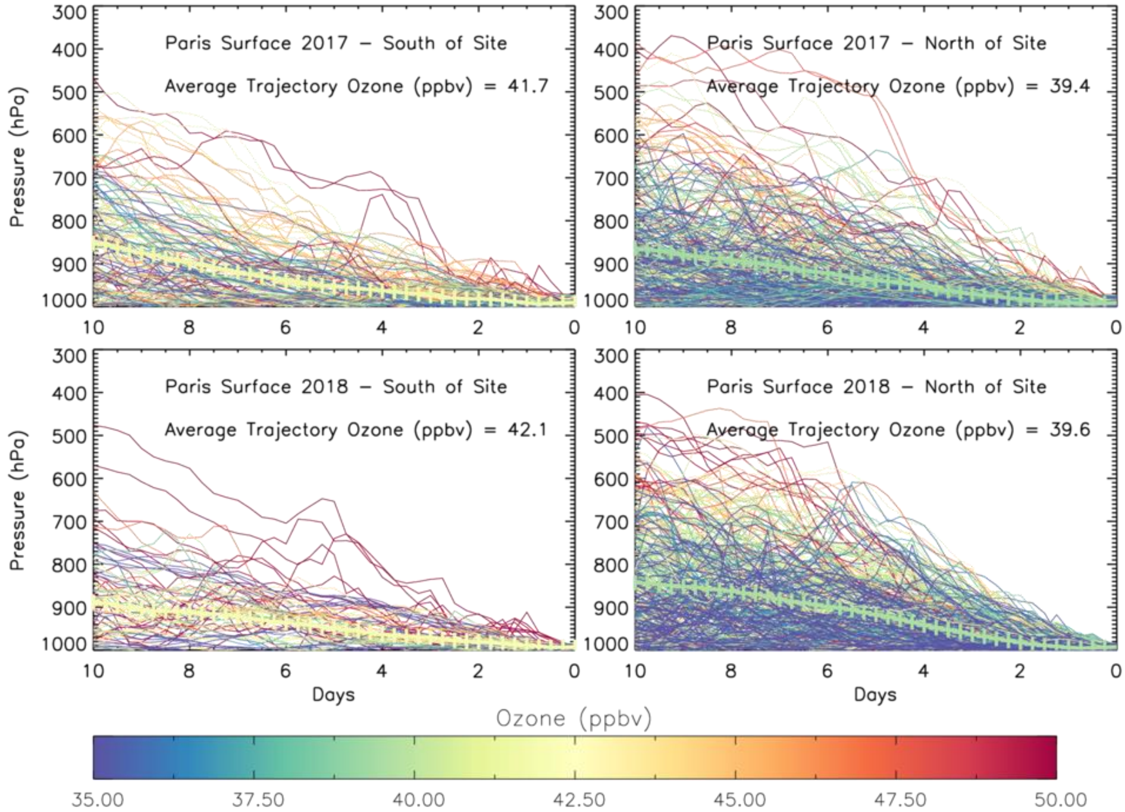

***Figure S18**: ROTRAJ back-trajectories (10 days), weighted by the average TOMCAT O_3 (ppbv) concentration along each trajectory path, plotted as time-pressure profiles, released from Paris near the surface for top-left) 2017 originating south of the release point, top-right) 2017 originating north of the release point, bottom-left) 2018 originating south of the release point and bottom-right) 2018 originating north of the release point. The thick cross lines show the average time-pressure profile coloured by the average weighted TOMCAT O_3 value.*

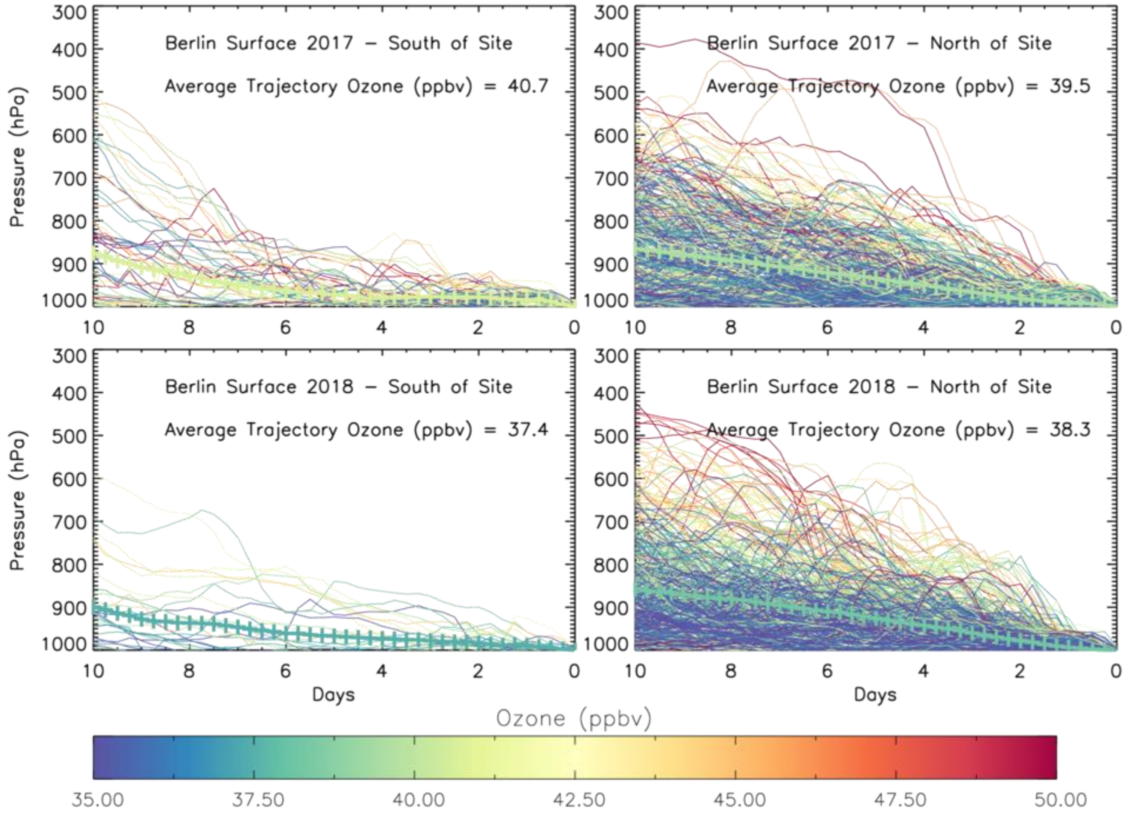

Figure S19*: ROTRAJ back-trajectories (10 days), weighted by the average TOMCAT O_3 (ppbv) concentration along each trajectory path, plotted as time-pressure profiles, released from Berlin near the surface for top-left) 2017 originating south of the release point, top-right) 2017 originating north of the release point, bottom-left) 2018 originating south of the release point and bottom-right) 2018 originating north of the release point. The thick cross lines show the average time-pressure profile coloured by the average weighted TOMCAT O_3 value.*

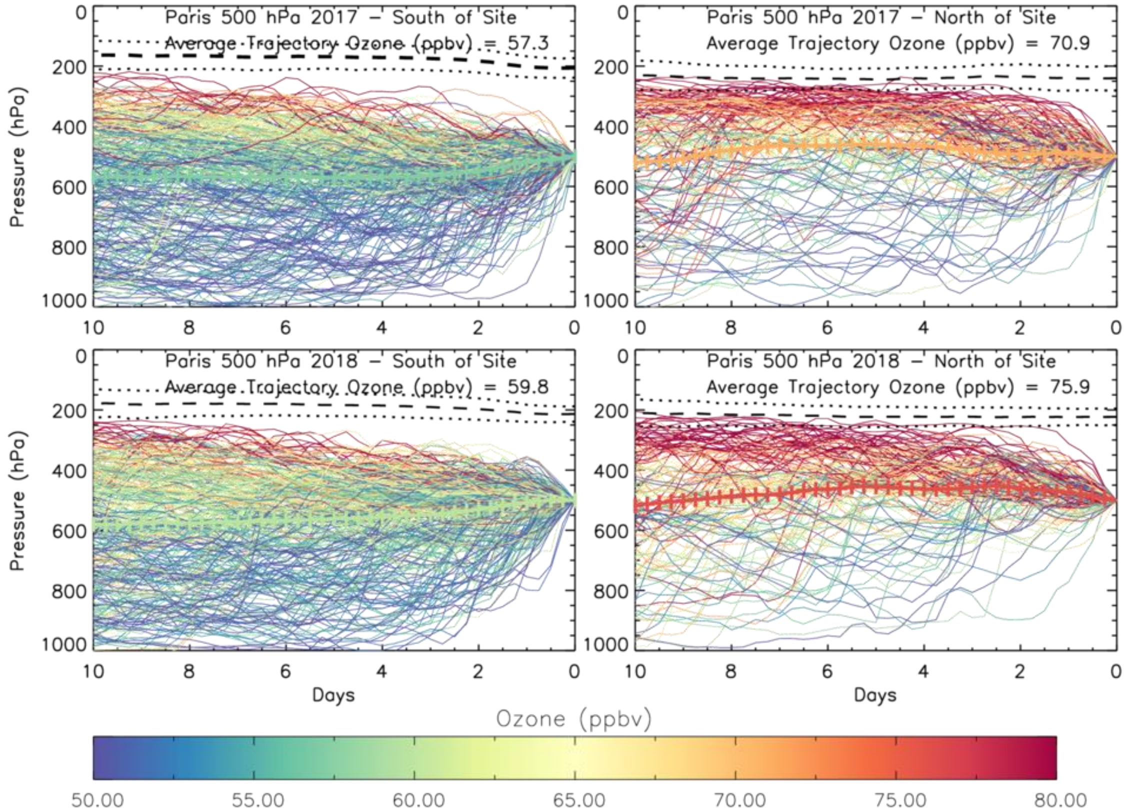

***Figure S20**: ROTRAJ back-trajectories (10 days), weighted by the average TOMCAT O_3 (ppbv) concentration along each trajectory path, plotted as time-pressure profiles, released from Paris at 500 hPa for top-left) 2017 originating south of the release point, top-right) 2017 originating north of the release point, bottom-left) 2018 originating south of the release point and bottom-right) 2018 originating north of the release point. The thick cross lines show the average time-pressure profile coloured by the average weighted TOMCAT O_3 value. The dashed black line presents the average tropopause pressure at each time-step of all the trajectories. The dotted black lines show the average tropopause pressure ± the standard deviation at each time step.*

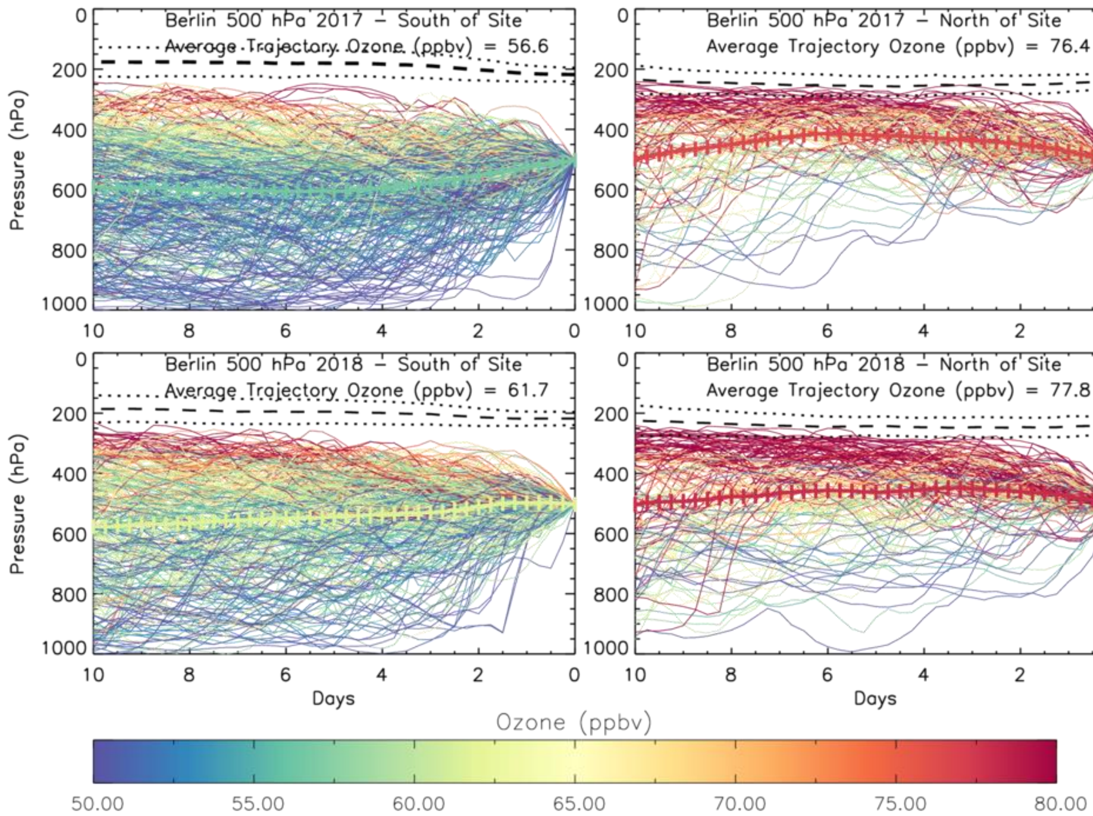

Figure S21: *ROTRAJ back-trajectories (10 days), weighted by the average TOMCAT* O_3 *(ppbv) concentration along each trajectory path, plotted as time-pressure profiles, released from Berlin at 500 hPa for top-left) 2017 originating south of the release point, top-right) 2017 originating north of the release point, bottom-left) 2018 originating south of the release point and bottom-right) 2018 originating north of the release point. The thick cross lines show the average time-pressure profile coloured by the average weighted TOMCAT* O_3 *value. The dashed black line presents the average tropopause pressure at each time-step of all the trajectories. The dotted black lines show the average tropopause pressure ± the standard deviation at each time step.*